EAI Endorsed Transactions
on Energy Web
Research Article EAI.EU

Capacity optimization of hybrid energy storage system considering battery loss

Hong Na[1,*], Jiacheng Wu[2], Guoping Lei[2], Jing An[2] and Xue He[1]

[1]Green Ecological Water Conservancy and Electric Power Engineering Research Center, Yunnan Water Resources and Hydropower Vocational College, Kunming 650499, China
[2]School of Electronic & Information Engineering, Chongqing Three Gorges University, Chongqing 404100, China

Abstract

INTRODUCTION: Wind power instability in microgrids impairs system economy, and rational hybrid energy storage system (HESS) capacity allocation is critical for mitigation.
OBJECTIVES: To address this, this study aims to optimize HESS configuration by minimizing battery loss and life cycle cost while ensuring stable operation.
METHODS: The approach involves: constructing a battery equivalent running time model via the rain-flow counting method, establishing a dual-objective optimization model, decomposing HESS suppression power into K intrinsic mode function(IMF) components using MISOA-VMD, and deriving optimal energy storage configurations and critical mode point with the NSGA-II algorithm.
RESULTS: Validation through comparative analysis of different schemes' minimum costs confirms the proposed scheme's superiority.
CONCLUSION: This study provides a reliable HESS configuration method to enhance the economy of wind power-integrated microgrids.

Keywords: HESS, rain-flow counting method, battery loss, life cycle cost, MISOA-VMD, NSGA-II algorithm, minimum full-life-cycle cost

Received on 05 November 2025, accepted on 12 December 2025, published on 31 March 2026

doi: 10.4108/ew.12034

*Corresponding author. Email: nahong@ynwateredu.com

1. Introduction

With the rapid integration of renewable energy sources like wind and solar power, the uncertainty, randomness, and intermittency of these energy outputs have become significant issues for the power grid [1,2]. Therefore, energy storage systems are crucial for addressing these challenges [3,4]. As single energy storage technology cannot meet the demands on the grid side, hybrid energy storage technology, which combines both energy-type and power-type storage components, offers flexible scheduling according to demand, thus enhancing system reliability. The larger the HESS capacity, the stronger its ability to stabilize grid fluctuations. However, increased capacity also leads to higher manufacturing costs, making the study of HESS capacity optimization highly significant [5].

Wei utilized the ensemble empirical mode decomposition method for total power decomposition of the hybrid storage system, aiming at minimizing the annual comprehensive cost of storage [6]. Wu proposed an improved wavelet packet decomposition method to decompose wind power, using a probability distribution function to fit and adjust the charging and discharging commands, thereby realizing capacity allocation of the hybrid energy storage system [7]. Liu proposed an enhanced adaptive noise complete

ensemble empirical mode decomposition method, which was applied to the capacity optimization of microgrid hybrid energy storage systems with the core objective of minimizing both initial investment and maintenance costs [8]. Dai adopted complete noise-assisted ensemble empirical mode decomposition for the decomposition of demand power, thereby realizing capacity optimization with the minimum comprehensive cost under constraints including the state of charge (SOC), capacity, and charging/discharging power of the energy storage system [9].

These studies mainly focused on the impact of power decomposition on the cost of hybrid energy storage capacity allocation [6-9]. Wei et al. optimized established models using intelligent optimization algorithms, while Cai decomposed target signals into high and low-frequency power demands using variational mode decomposition, with the goal of maximizing the net benefits of the hybrid energy storage system [10]. Deng used empirical mode decomposition for total output decomposition [11], and Lin put forward an improved local mean decomposition (ILMD) power distribution strategy and formulated an optimization model with the goal of minimizing life-cycle investment costs. Nevertheless, these studies have not adequately addressed the instability of renewable energy sources such as wind and solar energy [12]. Zhao proposed a HESS capacity optimization strategy considering SOC self-recovery to minimize storage configuration costs, establishing a lifecycle optimization configuration model for HESS [13]. Wu established a HESS capacity optimization model aiming at minimizing system costs, stabilizing renewable energy power fluctuations, and optimizing grid line utilization, ensuring reliable and economical microgrid operation [14]. Huang adopted the Analytic Hierarchy Process (AHP) to hierarchically decompose multi-objective functions into single-objective functions, thereby achieving the optimization of comprehensive economic and environmental benefits [15], while Wang proposed a model minimizing carbon trading and storage costs, startup/shutdown costs, wind curtailment costs, gas purchase costs, and more, verified through MATLAB and Gurobi solver [16].

Based on the above studies, this research constructs equivalent running time and battery loss models under the rain-flow counting method, with the objectives of minimizing life cycle cost and battery loss. Using MISOA-VMD for HESS power decomposition, the optimal critical mode point is treated as an optimization variable and solved using the NSGA-II algorithm. The superiority of the proposed configuration scheme is demonstrated through comparative analysis of different configurations.

2. Hybrid Energy Storage System Model Construction

2.1. Equivalent running time model under rain-flow counting method

Supercapacitors have characteristics of fast response and high cycle counts, with a lifespan much longer than that of batteries. Therefore, in this study, the equivalent lifespan of supercapacitors is fixed at 20 years, considering only the impact of battery cycle life on HESS capacity allocation.

Let the depth of discharge of the battery be C_{depth}, and the maximum number of cycles be $N_{\max}$. The battery's equivalent cycle count under complete charge-discharge conditions can be expressed:

$$\alpha(x)=\frac{N_{\max}}{N(C_{depth})} \tag{1}$$

In the formula, $N(C_{depth})$ and $\alpha(x)$ respectively represent the number of cycles corresponding at the current of C_{depth} and the number of cycles under full charge and discharge conditions at the current of C_{depth}.

Assuming the number of cycles per day is m, and the depth of discharge for each cycle is 1,2,3,…,m, the equivalent number of cycles per day for the battery can be expressed as:

$$N^{'}=\sum_{j=1}^{m}\alpha(x_j) \tag{2}$$

The calculation formula for the equivalent operating time of the battery is:

$$T_{equ}^{B}=\frac{N_{\max}}{365N^{'}} \tag{3}$$

2.2. Battery degradation model

This paper establishes a battery life degradation model related to capacity based on power fluctuations and power throughput over a period of time.

When the input and output power of the battery fluctuates drastically, it increases the battery life degradation. By increasing the battery capacity, the life degradation can be effectively reduced. The battery life degradation function caused by power fluctuations is expressed as follows:

$$L_{loss\_p_1}=\frac{\sum_{t=1}^{T}(P_b(t)-P_b(t-1))^2}{E_B} \tag{4}$$

In the formula, $P_b(t)$ is the battery's charging and discharging power at time T, T is the complete working condition time of 360 seconds; E_b is the battery's rated capacity.

Pang evaluates the number of battery charge and discharge cycles by calculating the ratio of the total power "throughput" of the battery over the complete working condition time to the total battery capacity, and then represents the battery life degradation by the ratio to the total discharge cycles D [17]. When the battery operates at

25°C and the depth of discharge is 0.6, the number of charge and discharge cycles is approximately 5000 times [18]. The established battery life degradation function is expressed as follows:

$$L_{loss\_p_2} = \frac{\int_0^T |P_b(t)|\,dt}{E_B D} \tag{5}$$

The weight of battery life degradation caused by power fluctuations is 0.6, and the weight of life degradation caused by power throughput is 0.4. The overall battery life degradation function is established as follows:

$$L_P = 0.6L_{loss\_p_1} + 0.4L_{loss\_p_2} \tag{6}$$

In this formula, a higher value represents greater battery degradation, while a lower value indicates less battery degradation.

3. Hybrid Energy Storage System Capacity Optimization Model and Solution

3.1. Objective function

(1) Objective 1: Minimizing the Life Cycle Cost (LCC) of HESS

The life cycle cost (LCC) calculation model of the hybrid energy storage system (HESS) comprehensively considers the total cost from investment and construction, operation and maintenance, to decommissioning and disposal of the storage system.The first objective is to minimize the annual comprehensive cost during the operation of the energy storage system, as expressed in the following formula:

$$f_1 = \min C_t = C_{iv} + C_{om} + C_{dc} \tag{7}$$

1) The total investment cost

$$C_{iv} = C_{biv} + C_{sciv} \tag{8}$$

The investment costs for the battery and the supercapacitor are denoted as C_{biv} and C_{sciv} respectively.

$$\begin{cases} C_{biv} = \dfrac{\delta(1+\delta)^{T_{equ}^B}}{(1+\delta)^{T_{equ}^B}-1}(C_{BP}P_B + C_{BE}E_B) \\ C_{sciv} = \dfrac{\delta(1+\delta)^{T_{equ}^{SC}}}{(1+\delta)^{T_{equ}^{SC}}-1}(C_{SCP}P_B + C_{SCE}E_{SC}) \end{cases} \tag{9}$$

Where C_{BP}, C_{BE}, C_{SCP} and C_{SEP} are the unit power cost and unit capacity cost of the battery and supercapacitor, while E_B, E_{SC} and P_B are the rated capacity and rated power of the battery and the battery supercapacitor, T_{equ}^B and T_{equ}^{SC} are the equivalent operating time of the battery and the supercapacitor, and δ is the discount rate.

2) Total operation and maintenance cost

$$C_{om} = C_{bom} + C_{scom} \tag{10}$$

The operation and maintenance costs of batteries and supercapacitors are as follows:

$$\begin{cases} C_{bom} = \dfrac{\delta(1+\delta)^{T_{equ}^B}}{(1+\delta)^{T_{equ}^B}-1} E_B C_B^* \\ C_{scom} = \dfrac{\delta(1+\delta)^{T_{equ}^{SC}}}{(1+\delta)^{T_{equ}^{SC}}-1} E_{SC} C_{SC}^* \end{cases} \tag{11}$$

where C_B^* and C_{SC}^* are the unit O&M costs of batteries and supercapacitors respectively.

3) Total processing cost

$$C_{dc} = C_{bdc}E_B + C_{scdc}E_{SC} \tag{12}$$

where, C_{bdc} and C_{scdc} are unit disposal costs of batteries and supercapacitors.

(2) Goal 2: Minimum battery loss

The minimum of formula 6, that is, the minimum loss of the battery, is denoted as f_2, , so the objective function $\min_{OBJ}$ is expressed as:

$$\min_{OBJ} = f_1 + f_2 \tag{13}$$

3.2. Constraints

In the capacity optimization process of a hybrid energy storage system, it is crucial to constantly consider the constraints of charge/discharge power, capacity, and SOC (State of Charge).

(1) Capacity constraints of the energy storage system, which are:

$$\begin{cases} -E_B < E_B(t) < E_B \\ -E_{SC} < E_{SC}(t) < E_{SC} \end{cases} \tag{14}$$

(2) Power constraints of the energy storage system, which are:

$$\begin{cases} -P_B < P_B(t) < P_B \\ -P_{SC} < P_{SC}(t) < P_{SC} \end{cases} \tag{15}$$

(3) SOC (State of Charge) constraints of the energy storage system, which are:

$$\begin{cases} SOC_{B,\min} < SOC_B(t) < SOC_{B,\max} \\ SOC_{SC,\min} < SOC_{SC}(t) < SOC_{SC,\max} \end{cases} \tag{16}$$

In the equations, $SOC_{B,\min}$, $SOC_{B,\max}$ respectively represent the upper and lower limits of the battery SOC, $SOC_{SC,\min}$, $SOC_{SC,\max}$ respectively represent the upper and lower limits of the supercapacitor SOC.

3.3. Solution methods

Power allocation under MISOA-VMD

Variational Mode Decomposition (VMD) constitutes a signal processing technique specifically designed to decompose a target signal into multiple distinct modes, wherein each mode corresponds to a unique set of frequency components. VMD achieves signal decomposition by optimizing an energy function, minimizing the signal energy within each mode while preserving the signal's original characteristics [19-23]. To address the difficulty in selecting parameters K and α in VMD, this study employs a multi-strategy optimized SOA (Snake Optimization Algorithm). The strategies incorporated are as follows:

(1) Employing a reverse difference population mutation mechanism to enhance population quality before iteration.

(2) Integrating the position update formula from the Subtraction of Mean Optimization Algorithm.

(3) Reiterating the poorer performing 50% of individuals to avoid premature convergence.

Upon successful decomposition, the signal yields *k*modal components. The critical point *j* where mode mixing in the Hilbert marginal spectrum is minimal, serves as the boundary between high and low frequency components. The battery handles the low-frequency power smoothing task for *j* or less, while the supercapacitor manages the high-frequency power smoothing task for *j* or more. The reconstructed expression is:

$$\begin{cases} P_b = P_{low}(t) = \sum_{k=1}^{j} u_k \\ P_{sc} = P_{high}(t) = \sum_{k=j+1}^{k} u_k \end{cases} \tag{17}$$

The specific process is shown in Figure 1.

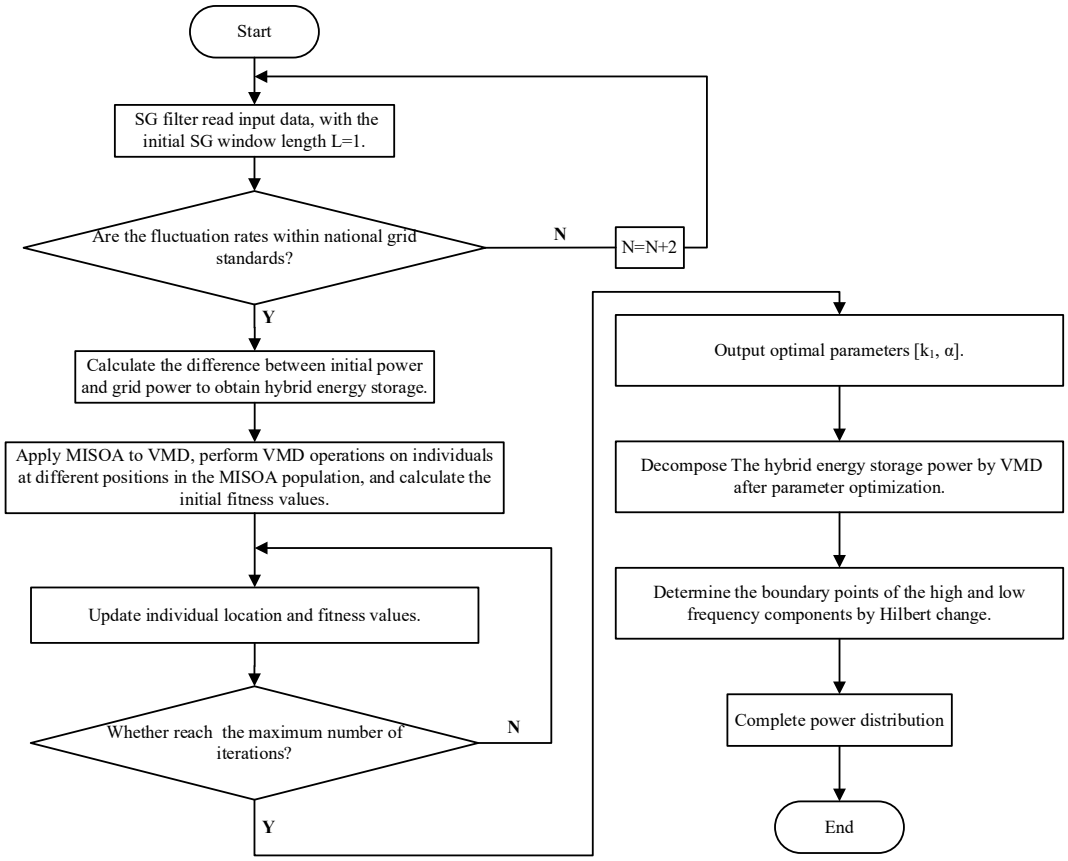

Figure 1. Flowchart of MISOA-VMD for power allocation

NSGA-II algorithm

To overcome the limitations of the Non-Dominated Sorting Genetic Algorithm (NSGA), Indian scientist Deb proposed an enhanced version in 2002 based on NSGA, known as the Elitist Non-Dominated Sorting Genetic Algorithm (NSGA-II). NSGA-II addresses the shortcomings of NSGA through the following improvements:

(1) Introduction of Fast Non-Dominated Sorting: NSGA-II introduced a fast non-dominated sorting algorithm to reduce the complexity of calculating non-dominated ranks. Fast non-dominated sorting categorizes the population into layers based on the individuals' non-dominated levels, guiding the search towards advancing Pareto-optimal solution sets.

Introduction of Crowding Distance and Crowding Distance Comparison Operator: To ensure a uniform distribution of solutions in the optimized objective space, the NSGA-II algorithm introduced the computation of crowding distance. The crowding distance $L(i)_d$ of each solution is calculated as the sum of distances to its adjacent two solutions along each optimization objective, which are:

$$L(i)_d = L(i)_d + \frac{(L[i+1]_m - L[i-1]_m)}{f_m^{\max} - f_m^{\min}} \quad (18)$$

In the equation, $L[i+1]_m$ translates to "the m-th objective function value of the (i+1)-th individual. $f_m^{\max}$ and $f_m^{\min}$ respectively denote the maximum and minimum values of the m-th objective function across the population.

(3) Introduction of elitist strategy, expanding the sampling space, and improving the accuracy of optimization results. The elitist strategy preserves excellent individuals from parents directly entering offspring to prevent loss of obtained Pareto optimal solutions and promote algorithm convergence.

When the overall life cycle cost reaches its optimum, the battery wear often cannot achieve the optimum, meaning two objective functions conflict with each other, making a unique solution impossible. Therefore, a compromise solution must be found in all Pareto sets, known as the Pareto front.

Algorithm steps are as follows:

Step 1. Within the range of satisfying the constraint bar square, generate random numbers to form the initial value of Pb, Eb, Psc and Esc;

Step 2. Adopt Formula 13 as the objective function, input the wind power mode components decomposed by Variational Mode Decomposition (VMD), calculate the fitness value of each individual in the population, subsequently perform fast non-dominated sorting on the individuals, compute the crowding degree of the population, and finally execute crossover operations to generate the individual members of the next-generation population.

Step 3. Determine whether the maximum number of iterations has been reached. If the condition is not satisfied, return to Step 1; if satisfied, output the Pareto Front.

3.4. Model solution

The solution of this life cycle model involves a nonlinear, multi-objective optimization problem [24]. In this study, the NSGA-II algorithm is employed to optimize energy storage configuration parameters while simultaneously determining the optimal critical mode points as optimization variables. Finally, the correctness of each critical mode point corresponding to its cost is validated. The specific process is shown in Figure 2.

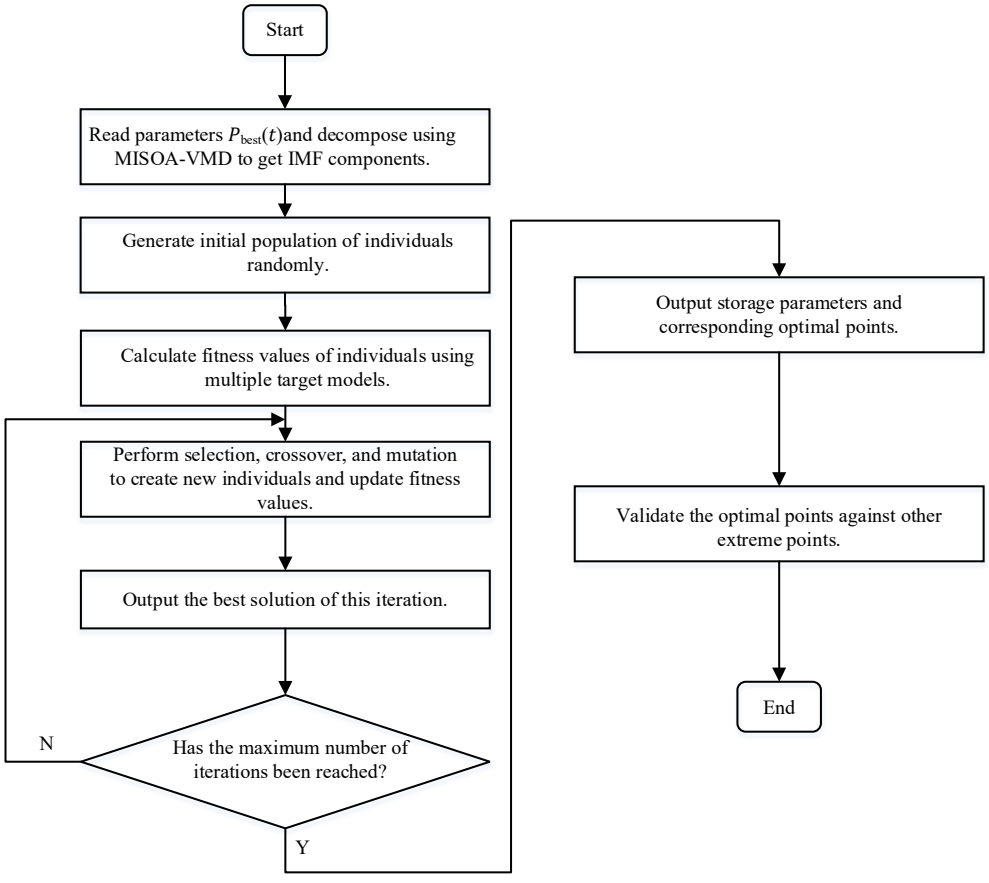

Figure 2. NSGA-II algorithm solution flowchart

4. Case Study Analysis

4.1. Case overview

This example uses data from a typical daily power generation of a 22 MW wind farm, sampled at 1-minute intervals. According to Chinese wind power grid integration standards, the maximum fluctuation limits for a 20 MW wind farm are 2 MW per minute and 6.6 MW per 10 minutes. The parameters related to the energy storage system are listed in Table 1.

Table 1. Energy Storage System Parameters

Performance Indicators	Battery	Supercapacitor
Unit Power Cost (million yuan/MWh)	270	150
Unit Capacity Cost (million yuan/MWh)	64	2700
Operation and Maintenance Cost (million yuan/MWh)	0.005	0.005
Processing Cost (million yuan/MWh)	-0.006	-0.007
State of Charge	0.2-0.9	0.1-0.9
Discount Rate δ	0.1	0.1
Rated Cycle Times (cycles)	350	\

Using the SG filtering algorithm to filter the original wind power, with a window length of N = 19, maximum fluctuations of 0.8894 MW and 5.1492 MW are obtained for 1-minute and 10-minute intervals, respectively, meeting China's grid power standards. The comparison results between the original power and the grid power are shown in Figure 3.

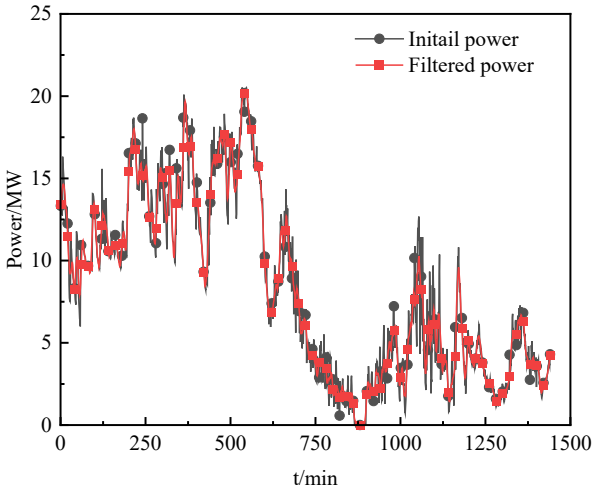

Figure 3. Comparison between original power and grid power

Applying the optimal parameter combination [10, 2164] iterated by the MISOA algorithm to VMD, 10 IMF components are obtained, as shown in Figure 4.

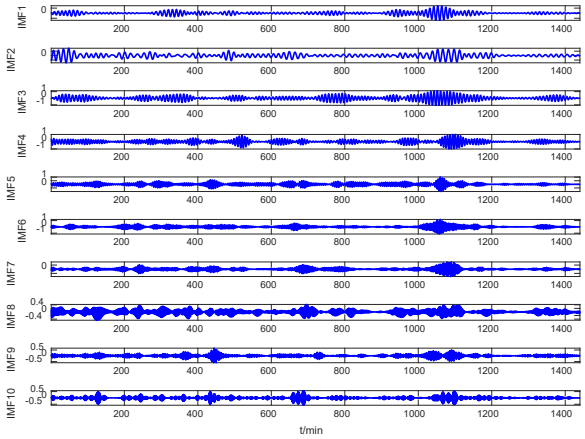

Figure 4. MISOA-VMD decomposition results

4.2. Capacity optimization results

Set the initial population number of NSGA-II algorithm as 50, and the number of iterations is 50. When the number of iterations is 50, the obtained solution tends to converge, and form the Pareto front composed of an optimal set, as shown in the red part of Figure 5.

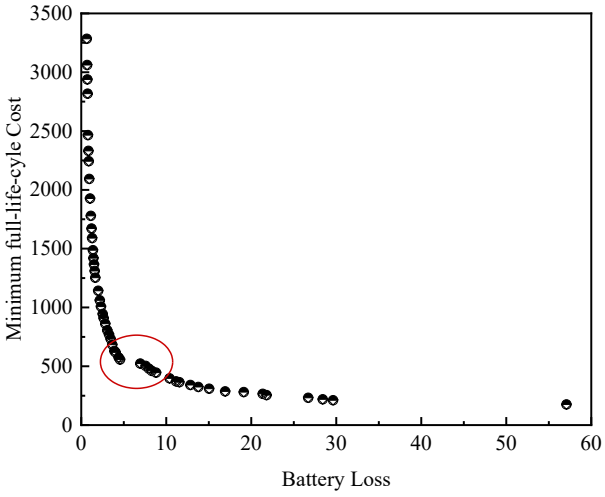

Figure 5. NSGA-II algorithm iteration convergence

To verify the effectiveness of the used MISOA-VMD power allocation method for the optimized configuration, the selected control group included single battery energy storage, single ultracapacitor energy storage, EMD based power decomposition energy storage, VMD based power decomposition energy storage. Due to a conflict between the two objectives of minimum battery loss and minimum full life cycle cost, making one objective function value smaller cannot make the other objective function value constant or

smaller. Therefore, Toppsis methods to select the optimal solution in the Pareto front [25], comparison diagram of rated power and rated capacity configuration results of battery and supercapacitors are shown in Figure 6 and Figure 7. The minimum cost and battery loss corresponding to different configuration modes are shown in Table 2.

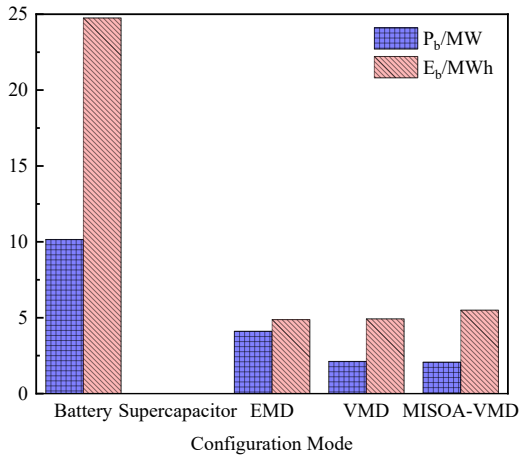

Figure 6. Comparison figure of battery parameters configuration

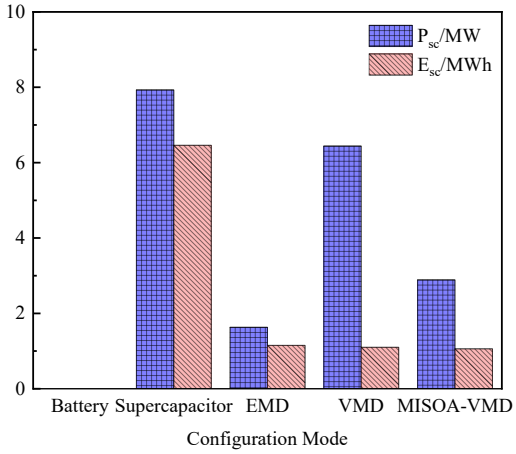

Figure 7. Comparison of the configuration of the supercapacitor parameters

Table 2. Cost and battery loss corresponding to the different configurations

Parameter\Configuration Mode	Battery	Supercapacitor	EMD	VMD	MISOA-VMD
C_t/million yuan	1623.41	2187.34	1583.24	828.86	696.02
Battery loss	\	\	16.79	9.72	8.48

As can be seen from FIG. 6 and 7, the rated power and rated capacity of batteries under MISOA-VMD decreased by about 80% and 78% respectively compared with the energy storage configuration of a single battery, Compared to the energy storage configuration of EMD power decomposition, Battery rated power configuration has decreased by about 50%, Rated capacity configuration was increased by approximately 11%, Compared to the VMD power decomposition, the rated power of the storage configuration decreased by about 2%, Rated capacity configuration is increased by about 10%, This is because when the battery assumes all the high-frequency power as an energy storage system, The rated power and rated capacity of ultraccapacitors at MISOA-VMD decreased by about 64% and 84% respectively compared to the energy storage configuration of single ultracapacitors, Compared to the energy storage configuration of EMD power decomposition, Battery rated power configuration is increased by about 44%, Rated capacity configuration decreased by about 8%, Compared with the VMD power decomposition of battery, the rated power of energy storage configuration has decreased by about 55%, Rated capacity configuration has decreased by about 4%.

It can be seen from Table 2 that the MISOA-VMD minimum cost is 57% lower than single battery energy storage configuration, 68% lower compared to single ultracapacitor energy storage configuration, 56% lower compared to EMD, and 16.02% lower compared to VMD. This result is because when the battery as an energy storage system need to bear all the high frequency power fluctuation, shorten the service life to improve the battery replacement cost, when the super capacitor as energy storage system, although can make up for the shortage of battery, but because of its low energy density, under the same energy storage requirements need to configure larger capacity, lead to increased costs. Similarly, MISOA-VMD improves its mode aliasing relative to EMD, and achieves accurate power allocation relative to VMD, thus reducing the whole life cycle cost. From the perspective of loss, the battery loss is about 78% lower than EMD power decomposition, and about 62% lower than VMD power decomposition mode.

4.3. Validation of optimal critical mode points

Under the MISOA-VMD configuration, the optimized critical point is 3.21, rounded up to the nearest whole number to obtain the optimal critical mode point of 4. Nine other critical points are calculated accordingly, as shown in Figure 8.

Table 3. Costs corresponding to different critical mode points

Critical Mode Point	C_t/million yuan
1	739.56
2	710.41
3	701.86
4	696.02
5	712.35
6	716.62
7	721.36
8	729.97
9	732.51
10	736.32

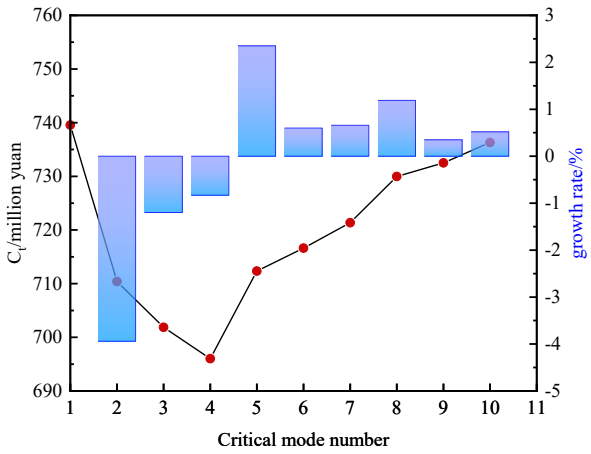

Figure 8. Different critical points correspond to costs and growth rates

By figure 8 in the demarcation point 4 to demarcation point 5 the corresponding growth rate from negative positive, the corresponding whole life cycle cost 6.9602 million yuan, and optimize the optimal critical mode point, the result is when the demarcation point selection is large, the battery bear more high frequency component, cycle life decline, increase the replacement cost of battery energy storage, make energy storage cost is high, when the demarcation point selection is small, most of the high frequency components will be by super capacitor response, which will increase the configuration requirements of super capacitor, and super capacitor monomer price expensive, large-scale configuration is unfavorable to the overall economy of HESS.

5. Conclusions

Addressing the capacity optimization problem of HESS composed of batteries and supercapacitors in wind power generation systems, this study utilized MISOA-VMD for power smoothing, established an equivalent operating time model for batteries using rainflow counting, and developed a battery loss model based on power fluctuations and throughput. The NSGA-II algorithm was employed with objectives to minimize the lifecycle cost and battery losses, while constraints included power, capacity, and SOC constraints of HESS. The optimal configuration of the hybrid energy storage system was achieved, with the optimal critical modal point treated as a variable in the optimization process. Case studies demonstrate that the proposed MISOA-VMD capacity configuration scheme outperforms single energy storage configurations, EMD power decomposition, and VMD power decomposition in terms of lifecycle cost and battery losses, yielding significant economic benefits.

However, the study has limitations. It only considered energy and power complementary storage devices. Future research should explore practical energy storage application scenarios and investigate various hybrid energy storage configurations to address these shortcomings.

Acknowledgements.

This research was funded by the Natural Science Foundation of Chongqing, China (No. CSTB2022NSCQ-MSX1320, CSTB2023NSCQ-LMX0027), the Project of Yunnan Water Resources and Hydropower Vocational College (No.2025YSZSYS003) and the Chongqing Wanzhou District Science and Technology Plan Project (No.wzstc20220301).

References

[1] Sun YS, Yang M, Shi ZL, et al. Analysis of the application status and development trend of energy storage. High Voltage Eng. 2020;46(1):80-89.

[2] Liu QH, Pang SM, Wu LL, et al. Mechanism, factors and impact law of voltage imbalance in large-scale wind power collection system. Trans China Electrotech Soc. 2022;37(21):5435-5450.

[3] Gu XP, Bai YS, Li SY, et al. Two-stage robust optimization method for power system restoration considering wind power uncertainty. Trans China Electrotech Soc. 2022;37(21):5462-5477.

[4] Silva MLSD, Wei P. Control strategy to smooth wind power output using battery energy storage system: A review. J Energy Storage. 2021;35.

[5] Liu YQ, Liang C, Yan J, et al. Optimal configuration and economic analysis of hybrid energy storage system in wind-solar power plants. Electr Power. 2020;53(12):143-150.

[6] Wei ZB, Yao YX, Zhang WW, et al. Capacity optimization configuration of hybrid energy storage system in microgrid based on complete ensemble empirical mode decomposition. Energy Storage Sci Technol. 2023;12(11):3414-3424.
[7] Wu X, Li YT, Ma ZY, et al. Capacity configuration method of hybrid energy storage system based on improved wavelet packet decomposition. Acta Energiae Solaris Sin. 2023;44(8):23-29.
[8] Liu XM, Zhang Y, Liu XB. Capacity configuration of microgrid hybrid energy storage based on ICEEMDAN. South Power Syst Technol. 2024.
[9] Dai SH, Wang KY, Cao B, et al. Optimal configuration of mixed energy storage capacity in thermal power plants based on CEEMDAN power decomposition. Trans China Electrotech Soc. 2024;19(1):57-66.
[10] Cai TT, Xue WD. Capacity optimization research of hybrid energy storage system for primary frequency regulation based on VMD. J Northeast Electr Power Univ. 2024;44(1):61-71.
[11] Deng K, Wen YJ, Hu P, et al. Study on capacity configuration of microgrid hybrid energy storage based on improved whale optimization algorithm. Intell Comput Appl. 2023;13(2):194-199.
[12] Lin JD, Zhu X, Shi XY, et al. Hybrid energy storage capacity optimization configuration based on improved LMD. J Fujian Univ Technol. 2024;22(1):39-46.
[13] Zhao JY, Qiao HP, Yao SL, et al. Strategy for hybrid energy storage capacity configuration considering SOC self-recovery of wind power fluctuation smoothing. Trans China Electrotech Soc. 2024.
[14] Wu CM, Yang ZH. Capacity optimization configuration of hybrid energy storage system based on improved whale algorithm. Electr Eng Mater. 2024;(1):84-89.
[15] Huang Z, Bei L, Wang B, et al. Capacity Optimization Configuration for a Park-Level Hybrid Energy Storage System Based on an Improved Cuckoo Algorithm. Processes. 2024;12(4).
[16] Wang C, Wang H, Ji X, et al. Hybrid energy storage capacity configuration strategy for virtual power plants based on variable-ratio natural gas-hydrogen blending. Int J Hydrogen Energy. 2024;58433-445.
[17] Pang S, Yang CP, Liu RL, et al. Multi-objective optimization method for capacity configuration of lithium battery energy storage system in ship microgrid. Chin J Ship Res. 2020;15(6):22-28.
[18] Jin WH, Liu JC. Capacity optimization configuration of hybrid energy storage system for smoothing wind power fluctuation. Distrib Energy. 2017;2(2):32-38.
[19] Kumar A, Rathore A. Modelling and testing of wind energy fed hybrid battery-supercapacitor energy storage operating in pulsed charging mode. Wind Eng., 2024; 48(2): 228-242.
[20] Zehua C, Kuan Z, Liyuan Y, et al. ANFIS based sound vibration combined fault diagnosis of high voltage circuit breaker (HVCB). Energy Rep., 2023; 9(S3): 286-294.
[21] Saeid H, Dylan RM. Low-power Spiking Neural Network audio source localisation using a Hilbert Transform audio event encoding scheme. Commun. Eng., 2025; 4(1): 18-18.
[22] Li J, Zhang Y, Wang H, et al. Optimal Design of a Hybrid Energy Storage System in a Plug-In Hybrid Electric Vehicle for Battery Lifetime Improvement. IEEE Trans. Transp. Electrif., 2025; 11(3): 4567-4578.
[23] Wang L, Chen Y, Zhang Q, et al. A Bi-Level Capacity Configuration Model for Hybrid Energy Storage Considering SOC Self-Recovery. Energy Rep., 2025; 11: 890-902.
[24] Zhang H, Liu S, Li M, et al. Capacity Optimization of Wind-PV-HESS for Buildings Considering Battery Life Loss. J. Clean. Prod., 2024; 420: 138654.
[25] Chen W, Zhao J, Yang Z, et al. Multi-Objective Sizing Optimization of Hybrid Energy Storage System Considering Battery Degradation in Microgrids. Appl. Energy, 2023; 345: 121234.